



## Interplay of quasiparticle and vibrational excitations: First observation of isomeric states in $^{168}\text{Dy}$ and $^{169}\text{Dy}$



G.X. Zhang<sup>a</sup>, H. Watanabe<sup>a,b,\*</sup>, G.D. Dracoulis<sup>c,1</sup>, F.G. Kondev<sup>d</sup>, G.J. Lane<sup>c</sup>, P.H. Regan<sup>e,f</sup>, P.-A. Söderström<sup>b</sup>, P.M. Walker<sup>e</sup>, K. Yoshida<sup>g</sup>, H. Kanaoka<sup>h</sup>, Z. Korkulu<sup>i</sup>, P.S. Lee<sup>j</sup>, J.J. Liu<sup>k</sup>, S. Nishimura<sup>b</sup>, J. Wu<sup>b,l</sup>, A. Yagi<sup>h</sup>, D.S. Ahn<sup>b</sup>, T. Alharbi<sup>m</sup>, H. Baba<sup>b</sup>, F. Browne<sup>n</sup>, A.M. Bruce<sup>n</sup>, M.P. Carpenter<sup>d</sup>, R.J. Carroll<sup>e</sup>, K.Y. Chae<sup>o</sup>, C.J. Chiara<sup>p,2</sup>, Zs. Dombradi<sup>i</sup>, P. Doornenbal<sup>b</sup>, A. Estrade<sup>q</sup>, N. Fukuda<sup>b</sup>, C. Griffin<sup>q</sup>, E. Ideguchi<sup>r</sup>, N. Inabe<sup>b</sup>, T. Isobe<sup>b</sup>, S. Kanaya<sup>h</sup>, I. Kojouharov<sup>s</sup>, T. Kubo<sup>b</sup>, S. Kubono<sup>b</sup>, N. Kurz<sup>s</sup>, I. Kuti<sup>i</sup>, S. Lalkovski<sup>e</sup>, T. Lauritsen<sup>d</sup>, C.S. Lee<sup>j</sup>, E.J. Lee<sup>o</sup>, C.J. Lister<sup>d</sup>, G. Lorusso<sup>b,e,f</sup>, G. Lotay<sup>e</sup>, E.A. McCutchan<sup>d</sup>, C.-B. Moon<sup>t</sup>, I. Nishizuka<sup>u</sup>, C.R. Nita<sup>n,v</sup>, A. Odahara<sup>h</sup>, Z. Patel<sup>e</sup>, V.H. Phong<sup>b,w</sup>, Zs. Podolyák<sup>e</sup>, O.J. Roberts<sup>x</sup>, H. Sakurai<sup>b</sup>, H. Schaffner<sup>s</sup>, D. Seweryniak<sup>d</sup>, C.M. Shand<sup>e</sup>, Y. Shimizu<sup>b</sup>, T. Sumikama<sup>u</sup>, H. Suzuki<sup>b</sup>, H. Takeda<sup>b</sup>, S. Terashima<sup>a</sup>, Zs. Vajta<sup>i</sup>, J.J. Valiente-Dóbon<sup>y</sup>, Z.Y. Xu<sup>k</sup>, S. Zhu<sup>d</sup>

<sup>a</sup> IRCNPC, School of Physics and Nuclear Energy Engineering, Beihang University, Beijing 100191, China

<sup>b</sup> RIKEN Nishina Center, 2-1 Hirosawa, Wako, Saitama 351-0198, Japan

<sup>c</sup> Department of Nuclear Physics, R.S.P.E., Australian National University, Canberra, ACT 2601, Australia

<sup>d</sup> Physics Division, Argonne National Laboratory, Argonne, IL 60439, USA

<sup>e</sup> Department of Physics, University of Surrey, Guildford GU2 7XH, United Kingdom

<sup>f</sup> National Physical Laboratory, Teddington, Middlesex, TW11 0LW, United Kingdom

<sup>g</sup> Department of Physics, Kyoto University, Kyoto, 606-8502, Japan

<sup>h</sup> Department of Physics, Osaka University, Machikaneyama-machi 1-1, Osaka 560-0043 Toyonaka, Japan

<sup>i</sup> MTA Atomki, P. O. Box 51, Debrecen, H-4001, Hungary

<sup>j</sup> Department of Physics, Chung-Ang University, Seoul 156-756, Republic of Korea

<sup>k</sup> Department of Physics, the University of Hong Kong, Pokfulam Road, Hong Kong

<sup>l</sup> Department of Physics, Peking University, Beijing 100871, China

<sup>m</sup> Department of Physics, College of Science in Zulfi, Majmaah University, Majmaah 11952, Saudi Arabia

<sup>n</sup> School of Computing, Engineering and Mathematics, University of Brighton, Brighton, BN2 4GJ, United Kingdom

<sup>o</sup> Department of Physics, Sungkyunkwan University, Suwon 440-746, Republic of Korea

<sup>p</sup> Nuclear Engineering Division, Argonne National Laboratory, Argonne, IL 60439, USA

<sup>q</sup> School of Physics and Astronomy, University of Edinburgh, Edinburgh EH9 3JZ, United Kingdom

<sup>r</sup> Research Center for Nuclear Physics (RCNP), Osaka University, Ibaraki, Osaka 567-0047, Japan

<sup>s</sup> GSI Helmholtzzentrum für Schwerionenforschung GmbH, 64291 Darmstadt, Germany

<sup>t</sup> Department of Display Engineering, Hoseo University, Chung-Nam 336-795, Republic of Korea

<sup>u</sup> Department of Physics, Tohoku University, Aoba, Sendai, Miyagi 980-8578, Japan

<sup>v</sup> Horia Hulubei National Institute for R & D in Physics and Nuclear Engineering (IFIN-HH), Bucharest-Magurele 077125, Romania

<sup>w</sup> VNU Hanoi University of Science, 334 Nguyen Trai, Thanh Xuan, Hanoi, Viet Nam

<sup>x</sup> School of Physics, University College Dublin, Belfield, Dublin 4, Ireland

<sup>y</sup> Istituto Nazionale di Fisica Nucleare, Laboratori Nazionali di Legnaro, 35020 Legnaro, Italy

### ARTICLE INFO

#### Article history:

Received 11 August 2019

Received in revised form 16 October 2019

Accepted 16 October 2019

### ABSTRACT

The neutron-rich dysprosium isotopes  $^{168}\text{Dy}_{102}$  and  $^{169}\text{Dy}_{103}$  have been investigated using the EURICA  $\gamma$ -ray spectrometer, following production via in-flight fission of a high-intensity uranium beam in conjunction with isotope separation through the BigRIPS separator at RIBF in RIKEN Nishina Center. For  $^{168}\text{Dy}$ , a previously unreported isomer with a half-life of 0.57(7)  $\mu\text{s}$  has been identified at an

\* Corresponding author at: Beihang University, 37 Xueyuan Road, Haidian District, Beijing 100191, P.R. China.

E-mail address: [hiroschi@ribf.riken.jp](mailto:hiroschi@ribf.riken.jp) (H. Watanabe).

<sup>1</sup> deceased.

<sup>2</sup> Present address: U.S. Army Research Laboratory, Adelphi, Maryland 20783, USA.

Available online 22 October 2019  
 Editor: D.F. Geesaman

excitation energy of 1378 keV, and its presence affirmed independently using  $\gamma$ - $\gamma$ - $\gamma$  coincidence data taken with Gammasphere via two-proton transfer from an enriched  $^{170}\text{Er}$  target performed at Argonne National Laboratory. This isomer is assigned  $J^\pi = K^\pi = (4^-)$  based on the measured transition strengths, decay patterns, and the energy systematics for two-quasiparticle states in  $N = 102$  isotones. The underlying mechanism of two-quasiparticle excitations in the doubly midshell region is discussed in comparison with the deformed QRPA and multi-quasiparticle calculations. In  $^{169}\text{Dy}$ , the  $B(E2)$  value for the transition de-exciting the previously unreported  $K^\pi = (1/2^-)$  isomeric state at 166 keV to the  $K^\pi = (5/2^-)$  ground state is approximately two orders of magnitude larger than the  $E2$  strength for the corresponding isomeric-decay transition in the  $N = 103$  isotone  $^{173}\text{Yb}$ , suggesting the presence of a significant  $\gamma$ -vibrational admixture with a dominant neutron one-quasiparticle component in the isomeric state.

© 2019 The Authors. Published by Elsevier B.V. This is an open access article under the CC BY license (<http://creativecommons.org/licenses/by/4.0/>). Funded by SCOAP<sup>3</sup>.

One of the fundamental and universal features of nuclear systematics observed across the chart of nuclides is that the nucleus incurs a deviation from the spherical equilibrium shape when increasing the proton/neutron valency moving away from the magic numbers. Rare-earth (RE) isotopes in the mass range from 150 to 180 are known to be well deformed even in their low-lying states. Despite the predicted smooth variation of axial deformation as a function of the proton number ( $Z$ ) or neutron number ( $N$ ) in the doubly midshell region [1–4], there are some irregularities in the systematics of the observed first  $2^+$  energies for even-even RE nuclides: local minima emerge at  $N = 98$  for  $^{62}\text{Sm}$ ,  $^{64}\text{Gd}$ ,  $^{66}\text{Dy}$  and at  $N = 104$  for Dy,  $^{68}\text{Er}$ ,  $^{70}\text{Yb}$  isotopes (see Fig. 30 in Ref. [5]). This anomalous behavior of the  $2^+$  energy has been discussed in terms of deformed sub-shell closures [6,7], which can stabilize the nuclear deformation and thereby have a significant impact on the formation of the so-called RE element peak around  $A = 165$  in the  $r$ -process solar abundance distribution [8,9]. The presence of energy gaps in the deformed single-particle space should also influence the excitation spectra in well-deformed nuclei, which are characterized by rotational and vibrational motion, as well as by other non-collective excitations like  $K$  isomers ( $K$  denotes the angular momentum projection on the symmetry axis of the deformed nucleus). The competition between such different intrinsic excitations makes the excited level structure more complicated than a simple coupling scheme predicts, due to possible configuration mixing. To provide a good testing ground for more advanced nuclear structure models that can be incorporated in any  $r$ -process network simulations, detailed spectroscopic studies of the excited states in this largely deformed region are highly demanded.

In this Letter, we present previously unreported isomeric states and their decay properties identified in  $^{168}\text{Dy}_{102}$  and  $^{169}\text{Dy}_{103}$ , which correspond to double- and single-hole systems relative to the valence maximum nucleus  $^{170}\text{Dy}$  located at the double midshell  $Z = 66$  and  $N = 104$ . The presence of isomers with half-lives of the order of several tens of nanoseconds or longer often facilitates exploration of exotic nuclei produced in fragment separators by measuring delayed  $\gamma$ -rays that are coincident with the identified particles on an event-by-event basis [10], as demonstrated recently for a number of neutron-rich RE isotopes at the Radioactive-Isotope Beam Factory (RIBF) [11–17]. Besides the usefulness to populate excited levels, characteristic isomers can serve as an effective probe for the underlying nuclear structure, such as single-particle orbitals, pairing correlations, and collective motions [18]. Thus, the present work can provide a significant insight into the structure of midshell nuclides that were hard to reach previously.

We have analyzed experimental data obtained from two independent experiments; one using the EURICA spectrometer at RIBF [19], and the other using the Gammasphere array at Argonne Tandem-Linac Accelerator System (ATLAS) facility [20]. At RIBF, neutron-rich nuclides around  $A = 170$  were produced by in-flight

fission of a  $^{238}\text{U}^{86+}$  beam at 345 MeV/u with an average intensity of 12 pnA, incident on a 5-mm thick Be target. The nuclei of interest were separated and identified through the in-flight separator BigRIPS [21]. Identification of particles with the atomic number ( $Z$ ) and the mass-to-charge ratio ( $A/Q$ ) was achieved on the basis of the  $\Delta E$ -TOF- $B\rho$  method, in which the energy loss ( $\Delta E$ ), time of flight (TOF), and magnetic rigidity ( $B\rho$ ) were measured using the focal-plane detectors on the beam line. In total about 1500, 9000, 3600, and 1700 ions were collected for  $^{168}\text{Dy}^{66+}$ ,  $^{168}\text{Dy}^{65+}$ ,  $^{169}\text{Dy}^{66+}$ , and  $^{169}\text{Dy}^{65+}$ , respectively, all of which were involved in the present data analysis. The identified particles were implanted into WAS3ABi [19], which consisted of two double-sided silicon-strip detectors (DSSSD) stacked compactly. Each DSSSD had a thickness of 1 mm with an active area segmented into 60 and 40 strips (1-mm pitch) on each side in the horizontal and vertical dimensions, respectively. The DSSSDs also served as detectors for electrons following  $\beta$ -decay and internal conversion processes [22]. Gamma rays emitted following the heavy-ion implantation and their subsequent radioactive decay were detected by the EURICA  $\gamma$ -ray spectrometer [19,23], consisting of 12 Cluster-type detectors, each of which contained seven HPGe crystals packed closely. More detailed information on the experimental setup and data analysis can be found in Ref. [5].

In the experiment at ATLAS, excited states in  $^{168}\text{Dy}$  were populated via two-proton removal from an  $^{170}\text{Er}$  target, bombarded by a  $^{136}\text{Xe}$  beam at 830 MeV. The target was composed of a 6 mg/cm<sup>2</sup> metallic foil, enriched in  $^{170}\text{Er}$ , and placed on a gold backing with a thickness of 25 mg/cm<sup>2</sup>, thick enough to stop the reaction products at the target position. Under these conditions, the effective beam energy ranges from about 20% above the Coulomb barrier at the entrance to near the barrier at the rear of the target. Gamma rays were detected with the Gammasphere array [20]. More detailed descriptions of the experimental conditions are presented in Ref. [24]. Gamma-ray coincidence measurements with a requirement that three or more Ge detectors fired, in conjunction with pulsed beams separated by 825 ns, complemented the results obtained at RIBF for isomers with half-lives in the nanosecond to microsecond range.

The level schemes of  $^{168}\text{Dy}$  and  $^{169}\text{Dy}$  established in the present work are displayed in Fig. 1, where the levels assigned different  $K^\pi$  quantum numbers are described in different colors. The reader is referred to the online version of this article.

Prior to the present work, the excited states of  $^{168}\text{Dy}$  had been studied by the  $\beta$  decay of  $^{168}\text{Tb}$  [27] and multi-nucleon transfer reactions with a  $^{82}\text{Se}$  beam incident on an  $^{170}\text{Er}$  target [28]. The  $\gamma$  rays at energies of 75 and 173 keV, which were previously assigned as  $(2_1^+) \rightarrow 0_1^+$  and  $(4_1^+) \rightarrow (2_1^+)$ , respectively, have been confirmed in delayed coincidence with  $^{168}\text{Dy}$  ions in the EURICA experiment, as shown in Figs. 2(a) and 2(b). In this analysis for isomeric-decay transitions, however, the 227-keV  $\gamma$  ray reported

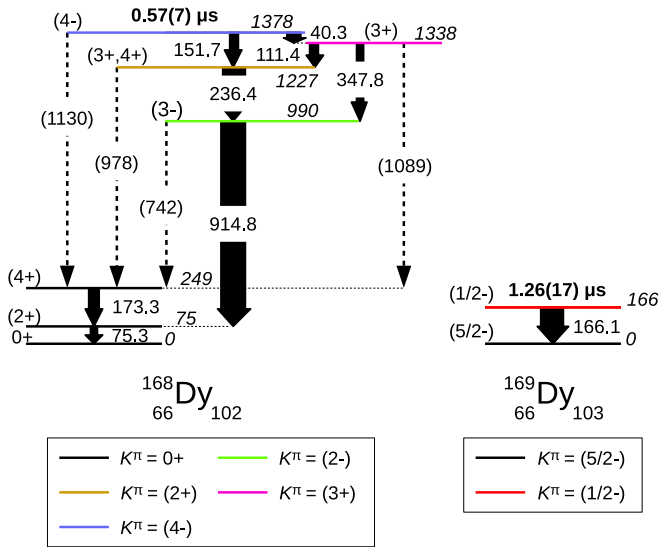


**Fig. 1.** Partial level schemes of  $^{168}\text{Dy}$  (left) and  $^{169}\text{Dy}$  (right) obtained in the present work. Each level is labeled with the spin-parity ( $J^\pi$ ) and energy values. The measured (isomeric) half-lives are indicated in bold. For  $^{168}\text{Dy}$ , the widths of solid arrows are proportional to the  $\gamma$ -ray relative intensities summarized in Table 1, while the dashed arrows represent possible (unobserved) transitions to account for the observation of the 173-keV,  $(4^+) \rightarrow (2^+)$   $\gamma$  ray (see text). Levels with different  $K^\pi$  quantum numbers are displayed in different colors, as indicated below each level scheme.

in Ref. [27] and the yrast  $E2$  sequence above the  $(4_1^+)$  state of the ground-state rotational band identified in Ref. [28] have not been observed, due presumably to the difference in feeding pattern. Meanwhile, two previously unreported  $\gamma$  rays at 915 and 236 keV can be unambiguously seen in Fig. 2(a).

The coincidence spectrum with a double gate on the 915- and 236-keV  $\gamma$  rays in the Gammasphere data [Fig. 2(c)] clearly exhibits  $\gamma$  rays at 111 and 152 keV, both of which are also visible in the low-energy part of the EURICA spectrum magnified in Fig. 2(b). Further analyses of the  $\gamma$ - $\gamma$ - $\gamma$  cubes reveal that the 111- and 152-keV transitions are *not* in mutual coincidence. Therefore, these transitions are placed in parallel with each other on top of the 236-915-keV cascade. Another previously unreported  $\gamma$  ray at 40 keV, which can be distinguished from the intense Dy  $K_{\alpha}$ -X rays, as demonstrated in Fig. 2(b), is assigned as feeding the 111-keV transition, since its energy perfectly matches the gap between the 152- and 111-keV  $\gamma$  rays. Similarly, a 348-keV  $\gamma$  ray, which was weakly populated in the EURICA experiment [see Fig. 2(a)], is placed in parallel with the 111- and 236-keV transitions.

In the EURICA experiment,  $\gamma$  rays following the  $\beta$  decay of  $^{168}\text{Tb}$  have also been observed with higher statistics than in Ref. [27]. The results of the  $\beta$ - $\gamma$  analysis will be presented elsewhere [26]. Here, for the sake of identification of the isomeric state in  $^{168}\text{Dy}$ , we use only the fact that the 915-keV  $\gamma$  ray is coincident with the 75-keV  $\gamma$  ray, but not with the 173-keV one [see Fig. 2(d)], thus being assigned as feeding the  $(2_1^+)$  state. An apparent  $\beta$  feeding to the 990-keV state from the parent nucleus  $^{168}\text{Tb}$ , which is expected to have a ground-state spin and parity of  $(4^-)$  with the  $\pi 3/2^+ [411] \otimes \nu 5/2^- [512]$  configuration [27], allows for a tentative assignment of  $J^\pi = (3^-)$  [26]. Note that the  $(4^-)$  assignment for  $^{168}\text{Tb}$  is based on the consideration of the spins and parities, as well as the corresponding Nilsson orbits, assigned to the respective ground states of the neighboring odd- $A$  Tb isotopes and  $N = 103$  isotones [27]. The negative-parity level in  $^{168}\text{Dy}$  is a candidate for the  $J^\pi = 3^-$  member of the  $K^\pi = 2^-$  octupole-vibrational band, which is known to emerge at compara-

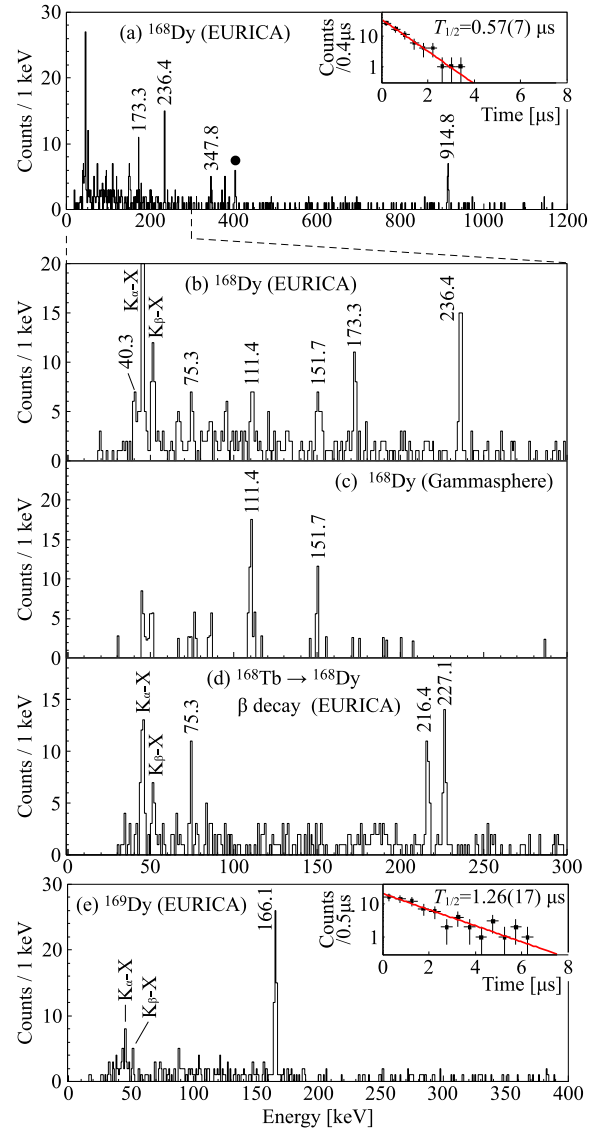


**Fig. 2.** (a) and (b): Gamma-ray energy spectra measured in EURICA after the implantation of  $^{168}\text{Dy}$  ions within a time range of 0.35 – 3  $\mu\text{s}$ . A contaminant (marked with a filled circle) arises from an isomeric state in  $^{173}\text{Ho}^{67+}$  [25], which can not be entirely separated from  $^{168}\text{Dy}^{65+}$  with respect to the atomic number on the particle-identification spectrum. Panel (b) magnifies the low-energy region up to 300 keV. The inset of panel (a) shows the sum of the time distributions of the 236- and 915-keV  $\gamma$  rays relative to the beam implantation. (c): Coincidence spectrum measured in Gammasphere with a double gate on the 236- and 915-keV  $\gamma$  rays in  $^{168}\text{Dy}$ . (d): Sum of coincidence spectra measured in EURICA with gates on the 915- and 216-keV  $\gamma$  rays following the  $\beta$  decay of  $^{168}\text{Tb}$  [26]. Transitions involved in the decay cascade are labeled with their energy values. (e): Energy projection obtained from the EURICA data in delayed coincidence with  $^{169}\text{Dy}$  ions within 0.35 – 6  $\mu\text{s}$ . The inset shows the time spectrum of the 166-keV  $\gamma$  ray.

tively low excitation energies ( $\lesssim 1.2$  MeV) in even- $A$  Dy isotopes with  $A = 160 - 166$  and 170 [14,29].

On the basis of the arguments presented above, a new isomeric state is identified at an excitation energy of 1378 keV in  $^{168}\text{Dy}$ . A half-life of 0.57(7)  $\mu\text{s}$  has been derived from a log-likelihood fit of the summed  $\gamma$ -ray gated time spectra for the isomeric-decay transitions, as shown in the inset of Fig. 2(a). The efficiency-corrected  $\gamma$ -ray intensities ( $I_\gamma$ ) relative to the 236-keV line are summarized in Table 1. It should be noted that, despite the observation of the 173-keV  $\gamma$  ray, any other  $\gamma$  rays which feed the  $(4_1^+)$  state can *not* be found in Fig. 2(a). If only one transition (e.g. an 1130-keV  $\gamma$  ray from the isomer) populated the  $(4_1^+)$  state, the total transi-

**Table 1**  
Summary of transitions from the  $K^\pi = (4^-)$  isomer in  $^{168}\text{Dy}$ .

$E_\gamma$ (keV)	$I_\gamma$ (rel.) <sup>a</sup>	$I_{\text{tot}}$ <sup>b</sup>	$\alpha_T^{\text{cal}}$ [30]	$\sigma\lambda$	$J_i^\pi \rightarrow J_f^\pi$	$F_W$ (W.u. <sup>-1</sup> )
40.3(3)	59(22)	97(36)	$6.5 \times 10^{-1}$	E1	$(4_1^-) \rightarrow (3_2^+)$	$3.8(19) \times 10^5$
75.3(3)	34(13)	304(122)	8.0	E2	$(2_1^+) \rightarrow 0_1^+$	
111.4(3)	39(15)	108(43)	1.8	M1	$(3_2^+) \rightarrow (3_1^+, 4_2^+)$	
151.7(3)	35(13)	38(14)	$1.0 \times 10^{-1}$	E1	$(4_1^-) \rightarrow (3_1^+, 4_2^+)$	$3.5(17) \times 10^7$
173.3(2)	52(18)	72(24)	$3.8 \times 10^{-1}$	E2	$(4_1^-) \rightarrow (2_1^+)$	
236.4(1)	100(30)	103(31)	$3.2 \times 10^{-2}$	E1	$(3_1^+, 4_2^+) \rightarrow (3_1^-)$	
347.8(5)	28(15)	29(16)	$1.2 \times 10^{-2}$	E1	$(3_2^+) \rightarrow (3_1^-)$	
914.8(3)	109(41)	109(41)	$1.5 \times 10^{-3}$	E1	$(3_1^-) \rightarrow (2_1^+)$	

<sup>a</sup> Relative to the  $\gamma$ -ray intensity of the 236-keV transition.

<sup>b</sup>  $I_{\text{tot}} = (1 + \alpha_T^{\text{cal}})I_\gamma$ .

tion intensity ( $I_{\text{tot}}$ ) would be balanced with the following 173-keV transition, yielding a peak area with  $\sim 10$  counts at the corresponding energy, enough to be observed in Fig. 2(a). Therefore, the non-observation of such connecting  $\gamma$  rays implies that the  $(4_1^+)$  state is populated via several transitions following the decay of the 1378-keV isomeric state.

For  $N = 102$  isotones,  $J^\pi = K^\pi = (4^-)$  isomers had been identified in  $^{170}\text{Er}$  ( $E_x = 1269$  keV,  $T_{1/2} = 43$  ns) [24] and  $^{172}\text{Yb}$  (1641 keV, 0.5 ns) [31], while  $J^\pi = K^\pi = (6^-)$  isomers identified in  $^{164}\text{Sm}$  (1486 keV, 0.6  $\mu\text{s}$ ),  $^{166}\text{Gd}$  (1601 keV, 0.95  $\mu\text{s}$ ) [11],  $^{170}\text{Er}$  (1591 keV, 4.0 ns) [24],  $^{172}\text{Yb}$  (1550 keV, 3.6  $\mu\text{s}$ ) [32], and  $^{174}\text{Hf}$  (1714 keV, 0.45 ns) [33]. The known  $K^\pi = (6^-)$  isomers decay either directly or indirectly towards the  $6^+$  state in the ground-state rotational band [29]. For  $^{168}\text{Dy}$ , since the previously reported  $(6_1^+) \rightarrow (4_1^+)$  transition of 268 keV [28] is not visible in Fig. 2(b) in spite of sufficiently low backgrounds, the 1378-keV isomeric state is unlikely to have  $K^\pi = 6^-$ , and therefore, assigned  $K^\pi = (4^-)$ .

The intensity of the 40-keV  $\gamma$  ray is compared to the sum of the total intensities of the subsequent 111- and 348-keV transitions in order to evaluate the total conversion coefficient  $\alpha_T$ . For all combinations of possible multiplicities of the 111- and 348-keV transitions, being either E1, M1, or E2, the deduced values of  $\alpha_T$  are in agreement only with a theoretical prediction for an E1 multipole character ( $\alpha_T^{\text{cal}} = 0.65$  [30]) within experimental errors. Therefore, the 40-keV transition is assigned as an E1 branch from the isomeric state at 1378 keV. The hindrance factor  $F_W$ , the inverse of the transition strength in Weisskopf units (W.u.), is evaluated to be  $3.8(19) \times 10^5$  for the 40-keV E1 transition. This value is consistent with those reported for the  $K_i^\pi = 4^- \rightarrow K_f^\pi = 3^+$  ( $\Delta K = 1$ ) transitions in the heavier  $N = 102$  isotones  $^{170}\text{Er}$  and  $^{172}\text{Yb}$  [34], supporting the  $J^\pi = K^\pi = (4^-)$  assignment for the 1378-keV isomeric state, which decays towards the  $K^\pi = (3^+)$  level at 1338 keV.

As will be discussed later, the  $K^\pi = (4^-)$  and  $(3^+)$  states in  $^{168}\text{Dy}$  are dominated by the  $\nu 1/2^- [521] \otimes \nu 7/2^+ [633]$  and  $\nu 5/2^- [512] \otimes \nu 1/2^- [521]$  configurations, respectively. Therefore, the  $K$ -allowed E1 transition between them is most likely ascribed to the single-neutron transition via  $\nu 7/2^+ [633] \rightarrow \nu 5/2^- [512]$  with the  $1/2^- [521]$  neutron being a spectator. For the  $K^\pi = 7/2^+$  and  $5/2^-$  levels at low excitation energy in the neighboring even- $Z$ ,  $N = 101$  and 103 nuclei, the corresponding E1 transitions are known to occur with hindrances  $F_W$  of the order of  $10^5 - 10^6$  [29], being consistent with the value obtained for the  $(4^-) \rightarrow (3^+)$  transition in  $^{168}\text{Dy}$ . This consistency in the transition strengths also supports the assignments for the  $K^\pi = (4^-)$  and  $(3^+)$  states.

The 1227-keV state prefers to decay towards the 990-keV state rather than the ground-state rotational band at lower excitation energy, implying that the 236-keV transition is of a fast E1 character. Such kind of ‘‘interband’’ E1 transitions have been known

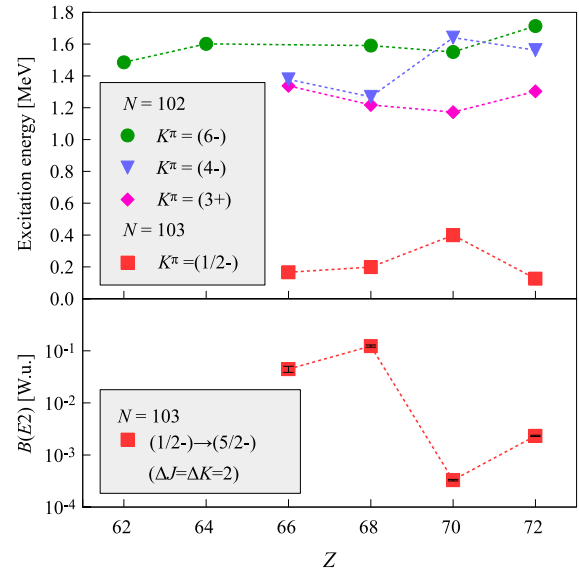


**Fig. 3.** Top: Excitation energies of the  $J^\pi = K^\pi = (6^-)$ ,  $(4^-)$ ,  $(3^+)$  states in  $N = 102$  and the  $(1/2^-)$  state in  $N = 103$  isotones. Bottom:  $B(E2)$  values in Weisskopf units (W.u.) of the  $(1/2^-) \rightarrow (5/2^-)$  transition with  $\Delta K = 2$  in  $N = 103$  isotones. The data are taken from the present work for  $^{168,169}\text{Dy}$  ( $Z = 66$ ) and from Ref. [29] for the others.

to take place between the  $K^\pi = 2^+$  ( $\gamma$ ) and  $K^\pi = 2^-$  (octupole) bands in the lighter even- $A$  Dy isotopes [29]. Therefore, the 1227-keV state is expected to have either  $J^\pi = 3^+$  or  $4^+$  with  $K^\pi = 2^+$ , which is populated via the 152-keV, E1 transition from the  $J^\pi = K^\pi = (4^-)$  isomeric state. The E1 hindrance  $F_W$  is about two orders of magnitude larger for the 152-keV branch than for the 40-keV transition, the other isomeric-decay branch towards the  $K^\pi = (3^+)$  state at 1338 keV (see Table 1). This is most likely ascribed to the difference in the  $K$  quantum number of the states to which the  $K^\pi = (4^-)$  isomer decays. Based on the consideration of the observed feeding pattern and hindrance, the 1227-keV state is associated with the  $K^\pi = (2^+)$   $\gamma$ -vibrational band.

The energy systematics of the  $J^\pi = K^\pi = (3^+)$ ,  $(4^-)$ , and  $(6^-)$  states observed for the  $N = 102$  isotones with  $Z = 62 - 72$  are shown in the upper panel of Fig. 3. They appear at excitation energies approximately equal to the pairing gap,  $2\Delta \sim 1.5$  MeV, in this mass region, being characteristic of two-quasiparticle (2qp) excitations in even-even nuclei that involve Nilsson orbits  $\Omega^\pi [Nn_z\Lambda]$  near the Fermi surface. It should be noted that a  $K^\pi = 6^-$  state has not been identified for  $^{168}\text{Dy}$  in the present work. That level is expected to emerge at around 1.6 MeV from the energy systematics, and to preferentially decay towards the lower-lying  $K^\pi = 4^-$  band with a short lifetime, as found for  $^{170}\text{Er}$  ( $T_{1/2} = 4$  ns) [24],



being presumably hard to observe with the present experimental sensitivity.

For  $^{169}\text{Dy}$ , no spectroscopic information had been reported before the present work. Fig. 2(e) exhibits a  $\gamma$ -ray energy spectrum measured in coincidence with the identified  $^{169}\text{Dy}$  ions within 0.35–6  $\mu\text{s}$ . A single  $\gamma$  ray observed at 166 keV can be interpreted as an E2 transition arising from a  $J^\pi = K^\pi = (1/2^-)$  isomer towards the presumed  $(5/2^-)$  ground state [see Fig. 1 (right)], in analogy with those identified before in the heavier  $N = 103$  isotones,  $^{171}\text{Er}$  ( $E_x = 199$  keV,  $T_{1/2} = 210$  ns),  $^{173}\text{Yb}$  (399 keV, 2.9  $\mu\text{s}$ ), and  $^{175}\text{Hf}$  (126 keV, 54  $\mu\text{s}$ ) [29]. A log-likelihood fit to the time distribution of the 166-keV  $\gamma$  ray yields  $T_{1/2} = 1.26(17)$   $\mu\text{s}$ , as shown in the inset of Fig. 2(d). The reduced transition probability for the presumed E2, 166-keV  $\gamma$  ray is evaluated to be  $B(E2; 1/2^- \rightarrow 5/2^-) = 2.5(3)$   $\text{e}^2\text{fm}^4 = 4.5(6) \times 10^{-2}$  W.u. by taking into account the competing internal conversion process with a theoretical total conversion coefficient  $\alpha_T^{\text{cal}} = 0.44$  [30]. The energies of the  $(1/2^-)$  states and the  $B(E2)$  values in the  $N = 103$  isotones are plotted in the upper and lower panels of Fig. 3, respectively.

It is to be noted that, although the aforementioned spin-parity assignments rely on the level systematics and plausible arguments on the observed transition strengths and decay patterns, all the individual arguments are convincing and ensure the full picture.

The excitation energies of the  $K^\pi = (3^+)$  states in the  $N = 102$  isotones vary smoothly around 1.2 MeV with a minimum at  $Z = 70$ . To understand the underlying mechanism of the  $K^\pi = 3^+$  excitation from a microscopic viewpoint, we have performed model calculations based on a Skyrme energy-density-functional (EDF) in the same framework as that applied to the  $K^\pi = 2^+$   $\gamma$ -vibrational excitation in our previous work [4,13]. With the use of the SkM\* functional [35], the ground states are calculated by the Hartree-Fock-Bogoliubov (HFB) method, while the Quasiparticle Random-Phase Approximation (QRPA) is employed for the intrinsic excitations. The experimental level energies in the  $N = 102$  isotones are compared to the results of the HFB+QRPA calculation in the upper panel of Fig. 4, where the energy values are measured relative to the  $K^\pi = (3^+)$  state in  $^{168}\text{Dy}$  in order to highlight the variation in the excitation energy as a function of the proton number. It can be seen that the calculation satisfactorily reproduces the observed trend of the  $K^\pi = (3^+)$  energies. As demonstrated in the lower panel of Fig. 4, the  $\nu 5/2^- [512] \otimes \nu 1/2^- [521]$  component dominates the  $K^\pi = 3^+$  wave functions in the  $N = 102$  isotones considered here. The calculations indicate that the  $K^\pi = 3^+$  levels fall in energy towards  $Z = 70$  along with the increase in the amplitude squared of the  $\pi 5/2^+ [402] \otimes \pi 1/2^+ [411]$  and  $\pi 7/2^+ [404] \otimes \pi 1/2^+ [411]$  components. Thus, these proton 2qp components play a decisive role in changing the excitation energy of the  $K^\pi = 3^+$  state along the isotonic chain. The QRPA calculation predicts that the sum of the amplitudes of these proton 2qp components is 14% for  $^{172}\text{Yb}$ , consistent with the argument based on the experimental  $g_K$  value [36], while the  $K^\pi = 3^+$  state in  $^{168}\text{Dy}$  consists of a nearly pure  $\nu 5/2^- [512] \otimes \nu 1/2^- [521]$  configuration.

The trend that the proton 2qp admixture is less significant in  $^{168}\text{Dy}$  (and  $^{170}\text{Er}$ ) than in  $^{172}\text{Yb}$  can be understood as follows: according to the Nilsson diagram for this mass region, the position of the  $Z = 70$  Fermi level is located between the  $\pi 7/2^+ [404]$  and  $\pi 1/2^+ [411]$  orbitals, giving rise to the lowest-lying proton 2qp state. With decreasing proton number from 70 in the  $N = 102$  isotonic chain, the energy of this proton 2qp state relative to the  $\nu 5/2^- [512] \otimes \nu 1/2^- [521]$  neutron configuration should be increased, and whereby its contribution to the  $K^\pi = 3^+$  structure becomes smaller.

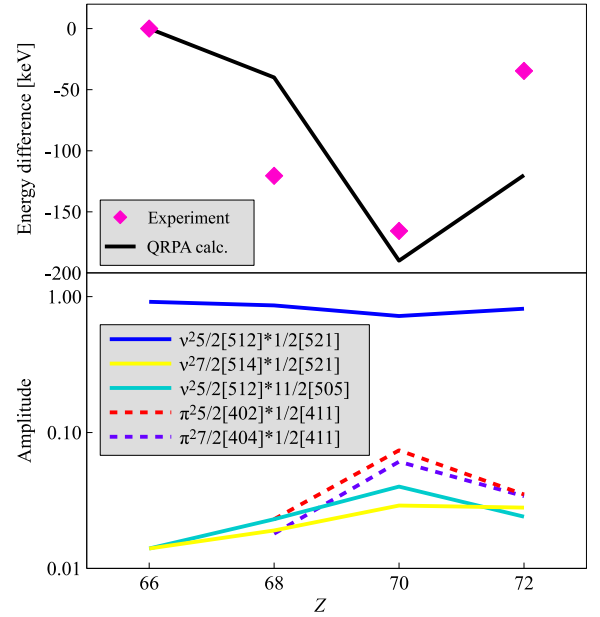
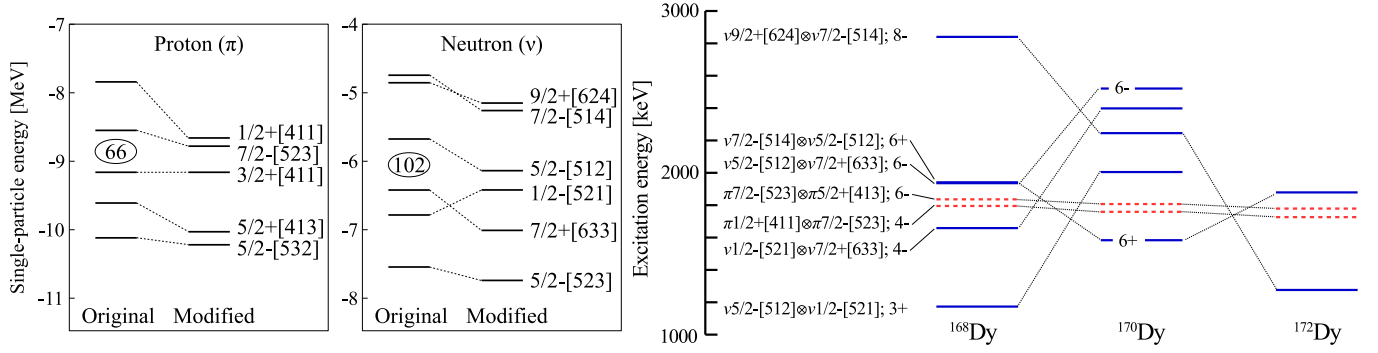


Fig. 4. Top: Energies of the  $K^\pi = (3^+)$  states in even- $A$   $N = 102$  isotones, relative to the level energy in  $^{168}\text{Dy}_{102}$ . The results of QRPA calculations using the SkM\* functional are also depicted by the thick solid line. Bottom: Amplitudes squared of the 2qp components in the QRPA wave functions for the  $K^\pi = 3^+$  excitation. The solid and dashed lines represent the neutron ( $\nu^2$ ) and proton ( $\pi^2$ ) components, respectively, which have the amplitudes larger than 0.01.

It is noteworthy that low-lying  $K^\pi = 3^+$  bands are systematically identified in even-even nuclei with  $N = 98 - 104$  and  $Z = 68 - 72$  [29], and that the  $J^\pi = 4^+$  members are strongly populated by deuteron and alpha inelastic scattering [37–39] that tends to favor collective excitations. The measured E4 strengths suggest the presence of hexadecapole vibrational nature [37–39].

In order to understand the  $K$  isomerism in the doubly mid-shell region, multi-quasiparticle calculations were performed for  $^{168,170,172}\text{Dy}$  in a similar way to an approach in Ref. [40], but with the inclusion of particle-number conservation by means of the Lipkin-Nogami prescription for the pairing correlations [41]. As the model implements the so-called “blocking effect”, the calculated pairing gaps and the Fermi level become configuration dependent. The energies and ordering of deformed single-particle (SP) levels were initially calculated based on the Woods-Saxon potential with universal parameters for fixed deformations  $\beta_2$ ,  $\beta_4$ , and  $\beta_6$  taken from Ref. [3], and then modified so as to reproduce approximately the empirical 1qp states in the neighboring odd- $A$  nuclei. The left part of Fig. 5 compares the original and modified SP energies around the  $Z = 66$  and  $N = 102$  Fermi surfaces. The most striking difference between the two sets of SP levels is the inversion of the  $\nu 1/2^- [521]$  and  $\nu 7/2^+ [633]$  orbits, which accounts for the appearance of the  $K^\pi = 3^+$  state at low excitation energy in the  $N = 102$  isotones, as discussed above. The rising of the  $\nu 1/2^- [521]$  level also causes a sizable gap at  $N = 98$  between the  $\nu 5/2^- [523]$  and  $\nu 7/2^+ [633]$  orbitals [7].

The results of the multi-quasiparticle calculations obtained with the modified SP levels are shown in the right part of Fig. 5. Here, the proton and neutron 2qp states were calculated independently, and subsequently corrected for the empirical residual interactions that depend on the configurations involved, i.e., the spin-singlet coupling is somewhat lowered in energy, while the energetically unfavored spin-triplet coupling is raised, following the Gallagher-Moszkowski rule [42]. The calculations suggest that there are two  $K^\pi = 4^-$  states with the  $\nu 1/2^- [521] \otimes \nu 7/2^+ [633]$  and  $\pi 1/2^+ [411] \otimes \pi 7/2^- [523]$  configurations. For  $^{168}\text{Dy}$ , these



**Fig. 5.** (Left): Deformed single-particle (SP) levels around the Fermi surfaces for  $Z = 66$  and  $N = 102$  obtained from the original set of the Nilsson orbits and modified so as to reproduce the experimental 1qp states in odd-mass nuclei in the region of interest. (Right): Excitation energy of 2qp states calculated by multi-quasiparticle calculations using the modified SP levels. Configurations and the resultant  $K^\pi$  values are indicated on the left-hand side of the excited levels. The neutron and proton 2qp levels are described by the blue solid and red dashed horizontal bars, respectively. The dotted lines connecting the levels with the same  $K^\pi$  configuration are a guide to the eye.

two configurations are expected to be strongly mixed since they are located in energy close to each other. (Such strong mixing between the two  $K^\pi = 4^-$  configurations was suggested to take place in the neighboring even- $Z$   $N = 102$  isotone  $^{170}\text{Er}$  based on the measured gyromagnetic ratios [24].) Using the calculated energy difference (137 keV) and the mixing matrix element derived from the  $^{170}\text{Er}$  case (190 keV [24]), the wave function, 67%  $\nu 1/2^- [521] \otimes \nu 7/2^+ [633] + 33\% \pi 1/2^+ [411] \otimes \pi 7/2^- [523]$ , is evaluated for one of the two mixed  $K^\pi = 4^-$  states at lower energy (specified as  $4_1^-$ ), which is associated with the 1378-keV isomeric state in  $^{168}\text{Dy}$ .

According to the calculations, there are two  $K^\pi = 6^-$  states with the  $\pi 7/2^- [523] \otimes \pi 5/2^+ [413]$  and  $\nu 5/2^- [512] \otimes \nu 7/2^+ [633]$  configurations above the  $4^-$  states in  $^{168}\text{Dy}$ . The neutron 2qp configuration was assigned to the  $K^\pi = 6^-$  isomers in the  $N = 102$  isotones,  $^{172}\text{Yb}$  [36],  $^{170}\text{Er}$  [24],  $^{166}\text{Gd}$  and  $^{164}\text{Sm}$  [11]. Similarly to the aforementioned  $K = 4^-$  case, these two  $K^\pi = 6^-$  components should be mixed with each other due to the proximity of their energies. It is expected that the mixed  $6_1^-$  state is higher in energy than the  $4_1^-$  state, consistent with the energy systematics shown in the upper panel of Fig. 3. The calculations also predict that the neutron 2qp excitations with  $K^\pi = 6^+$  ( $\nu 7/2^- [514] \otimes \nu 5/2^- [512]$ ) and  $K^\pi = 8^-$  ( $\nu 9/2^+ [624] \otimes \nu 7/2^- [514]$ ) emerge at relatively low excitation energies in  $^{170}\text{Dy}$  and  $^{172}\text{Dy}$ , respectively. They have been identified as a long-lived isomer in each Dy isotope [13,14], while the corresponding levels were not observed in  $^{168}\text{Dy}$ .

In  $^{169}\text{Dy}$ , the  $J^\pi = K^\pi = (1/2^-)$  state is interpreted as being predominantly of neutron 1qp nature, and its low excitation energy (166 keV) is ascribed to the rising of the  $\nu 1/2^- [521]$  level towards the  $\nu 5/2^- [512]$  one. This state becomes a long-lived isomer because, in addition to the small energy gap, the  $1/2^- \rightarrow 5/2^-$  “ $K$ -allowed”  $E2$  transition proceeds with changes in the asymptotic quantum numbers,  $[\Delta\Omega, \Delta N, \Delta n_z, \Delta\Lambda] = [2, 0, 1, 1]$  [43]. Indeed, the corresponding  $E2$  transition in the  $N = 103$  isotone  $^{173}\text{Yb}$  has the smallest  $B(E2)$  value observed to date in any odd- $A$  deformed nuclei [29]. As exhibited in the lower panel of Fig. 3, however, the  $B(E2)$  values in  $^{169}\text{Dy}$  and  $^{171}\text{Er}$  are more than two orders of magnitude larger than that of  $^{173}\text{Yb}$ . Note that the observed increase in  $B(E2)$  is in phase with a sudden fall of the  $\gamma$ -vibrational states in even- $A$  Dy and Er isotopes compared to the Yb levels, indicating that  $\gamma$ -vibrational motion is enhanced [13]. As such, in order to explain the increase of  $B(E2)$  in  $^{169}\text{Dy}$ , we consider states of mixed 1qp and  $\gamma$ -vibrational character. Based on the prescription described in Ref. [44], the wave functions of the  $1/2^-$  and  $5/2^-$  states can be described as

$$\begin{aligned} |1/2^- \rangle &= |\nu 1/2^- [521] \otimes 0_{\text{gs}}^+ \rangle + \alpha_{1/2} |\nu 5/2^- [512] \otimes 2_\gamma^+ \rangle, \\ |5/2^- \rangle &= |\nu 5/2^- [512] \otimes 0_{\text{gs}}^+ \rangle + \alpha_{5/2} |\nu 1/2^- [521] \otimes 2_\gamma^+ \rangle, \end{aligned}$$

where the  $|\nu \otimes 0_{\text{gs}}^+ \rangle$  and  $|\nu \otimes 2_\gamma^+ \rangle$  terms represent the coupling of a neutron 1qp state with the ground state and the  $K^\pi = 2^+$   $\gamma$ -vibrational excitation in the even-even core, respectively. The mixing coefficients  $\alpha_{1/2}, \alpha_{5/2} \ll 1$  are given by the perturbation theory as

$$\begin{aligned} \alpha_{1/2} &= -\frac{\langle \nu 5/2^- [512] \otimes 2_\gamma^+ | V | \nu 1/2^- [521] \otimes 0_{\text{gs}}^+ \rangle}{E_{2_\gamma^+} + E_{1\text{qp}}}, \\ \alpha_{5/2} &= -\frac{\langle \nu 1/2^- [521] \otimes 2_\gamma^+ | V | \nu 5/2^- [512] \otimes 0_{\text{gs}}^+ \rangle}{E_{2_\gamma^+} - E_{1\text{qp}}}, \end{aligned}$$

where  $E_{2_\gamma^+}$  and  $E_{1\text{qp}}$  in the denominators represent the excitation energy of the  $2_\gamma^+$  state and the energy difference between the (unperturbed)  $\nu 1/2^- [521]$  and  $\nu 5/2^- [512]$  levels, respectively. The numerators are the mixing matrix elements between the coupled states, which, for simplicity, are assumed to be equal to each other and denoted by  $\langle V \rangle$  in the following discussion. By omitting the cross term that contains the product of  $\alpha_{1/2}$  and  $\alpha_{5/2}$  in the  $E2$  matrix element, and using the single-particle and collective transition strengths, the reduced transition probability can be approximated as

$$\begin{aligned} B(E2; 1/2^- \rightarrow 5/2^-) &\approx \left[ \sqrt{B(E2; \nu 1/2^- \rightarrow \nu 5/2^-)} \right. \\ &\quad \left. + (\alpha_{1/2} + 1.73 \alpha_{5/2}) \sqrt{B(E2; 2_\gamma^+ \rightarrow 0_{\text{gs}}^+)} \right]^2. \end{aligned}$$

The values of  $B(E2; \nu 1/2^- \rightarrow \nu 5/2^-) = 1.88 \times 10^{-2} \text{ e}^2 \text{ fm}^4$  and  $E_{1\text{qp}} = 399 \text{ keV}$  are taken from the experimental data of  $^{173}\text{Yb}$  [29] since, as suggested in Ref. [45], the relative smallness of the  $E2$  matrix element between these states points to an almost total absence of  $\nu 5/2^- [512] \otimes 2_\gamma^+$  in the  $1/2^-$  band. As for the  $\gamma$ -vibrational core, the value of  $E_{2_\gamma^+}$  is estimated to be 1150 keV with the assumption that the observed 1227-keV state in  $^{168}\text{Dy}$  is the  $J^\pi = 3^+$  member of the  $\gamma$ -vibrational band, while  $B(E2; 2_\gamma^+ \rightarrow 0_{\text{gs}}^+) = 2.06 \times 10^2 \text{ e}^2 \text{ fm}^4$  is adopted from  $^{170}\text{Er}$  [29] that shows a similar enhancement of  $\gamma$  vibration. In consequence, the parameters  $\langle V \rangle = -34 \text{ keV}$ ,  $\alpha_{1/2} = 0.022$ ,  $\alpha_{5/2} = 0.045$  are obtained. It can be seen that a tiny ( $< 1\%$ ) admixture of  $\gamma$  vibration with the dominating neutron 1qp component enables the large increase in the  $E2$  strengths for the  $1/2^- \rightarrow 5/2^-$  transition.

The weak mixing phenomenon observed in the present work is at variance with the majority of data concerning the occurrence of  $\gamma$ -vibrational mixing in well-deformed odd- $A$  nuclides: the observed low-lying  $K = 1/2$  states of mixed 1qp-plus- $\gamma$ -vibrational character are in most cases found to contain appreciable admixtures of collective components [45]. For instance, approximately equal components of the admixed 1qp and  $\nu \otimes 2_{\gamma}^{+}$  configurations were suggested for the  $K^{\pi} = 1/2^{-}$  state at 707 keV in  $^{171}\text{Er}$  and the  $K^{\pi} = 1/2^{+}$  states at 581 keV in  $^{159}\text{Tb}$  and at 879 keV in  $^{183}\text{Re}$ . Such strong  $\gamma$ -vibrational mixing is known to occur with  $\langle V \rangle$  of the order of a few hundreds of keV, when the admixed 1qp excitation is connected to the “base” state, to which  $2_{\gamma}^{+}$  is coupled, by large (non-axial) quadrupole matrix elements, i.e., their asymptotic quantum numbers differ by  $\Delta\Omega = \Delta\Lambda = \pm 2$  with  $N$  and  $n_z$  unchanged.

To conclude, the excited states of  $^{168}\text{Dy}$  and  $^{169}\text{Dy}$ , which have two- and one-neutron vacancies relative to the doubly midshell nucleus  $^{170}\text{Dy}$ , have been populated following the decay from previously unreported isomeric states with half-lives of 0.57(7)  $\mu\text{s}$  and 1.26(17)  $\mu\text{s}$ , respectively. In  $^{168}\text{Dy}$ , the  $J^{\pi} = K^{\pi} = (4^{-})$  isomeric state at 1378 keV is expected to have a mixed proton and neutron 2qp configuration, while the HFB+QRPA calculation suggests that the  $J^{\pi} = K^{\pi} = (3^{+})$  level, which is located 40 keV below the isomer, is of nearly pure neutron 2qp nature. For  $^{169}\text{Dy}$ , the observed large enhancement of the  $B(E2)$  value for the  $(1/2^{-}) \rightarrow (5/2^{-})$  isomeric-decay transition over the corresponding transition in the heavier  $N = 103$  isotone  $^{173}\text{Yb}$  can be explained by configuration mixing between a dominating neutron 1qp component and  $\gamma$ -vibrational excitations in the  $K^{\pi} = (1/2^{-})$  isomeric state.

We are indebted to the facility crews who provided the beams at RIBF, cooperated by RIKEN Nishina Center and CNS, University of Tokyo, the EUROBALL Owners Committee for the loan of germanium detectors, and the PreSpec Collaboration for the use of the readout electronics. Part of the WAS3ABI was supported by the Rare Isotope Science Project which is funded by MSIP and NRF of Korea. This work was supported by JSPS KAKENHI Grant Nos. 24740188, 25247045, and 25287065, Science and Technology Facilities Council UK by Grant Nos. ST/L005743/1 and ST/P005314 (UK authors) and the UK National Measurement Office (PHR), the U.S. Department of Energy, Office of Science, Office of Nuclear Physics under Contract No. DE-AC02-06CH11357 (ANL), NRF Korea Grants No. 2017M2A2A6A02071071 and 2016R1D1A1A09917463 (CSL), 2014S1A2A2028636 and 2016K1A3A7A09005579 (KYC), Science Foundation Ireland under Grant No. 12/IP/1288 (OJR), Australian Research Council Grant No. FT100100991 (GJL), and Hungarian National Research and Innovation Office contract No. GINOP-2.3.3-15-2016-00034 (ZsD, IK, ZK). IK was supported by National Research, Development and Innovation Office-NKFIH, con-

tract No. PD 124717. The numerical calculations were performed on SR16000 at YITP, Kyoto University, and on COMA (PACS-IX) at CCS, University of Tsukuba. This research used resources of Argonne National Laboratory’s ATLAS facility, which is a DOE Office of Science User Facility.

## References

- [1] A.K. Rath, et al., *Phys. Rev. C* 68 (2003) 044315.
- [2] C.E. Vargas, V. Velázquez, S. Lerma, *Eur. Phys. J. A* 49 (2013) 1.
- [3] P. Möller, et al., *At. Data Nucl. Data Tables* 109–110 (2016) 1.
- [4] K. Yoshida, H. Watanabe, *Prog. Theor. Exp. Phys.* 2016 (2016) 123D02.
- [5] H. Watanabe, *Eur. Phys. J. A* 55 (2019) 19.
- [6] S.K. Ghorui, et al., *Phys. Rev. C* 85 (2012) 064327.
- [7] D.J. Hartley, et al., *Phys. Rev. Lett.* 120 (2018) 182502.
- [8] R. Surman, et al., *Phys. Rev. Lett.* 79 (1997) 1809.
- [9] M.R. Mumpower, G.C. McLaughlin, R. Surman, *Phys. Rev. C* 85 (2012) 045801.
- [10] T. Nakamura, H. Sakurai, H. Watanabe, *Prog. Part. Nucl. Phys.* 97 (2017) 53.
- [11] Z. Patel, et al., *Phys. Rev. Lett.* 113 (2014) 262502.
- [12] Z. Patel, et al., *Phys. Lett. B* 753 (2016) 182.
- [13] H. Watanabe, et al., *Phys. Lett. B* 760 (2016) 641.
- [14] P.-A. Söderström, et al., *Phys. Lett. B* 762 (2016) 404.
- [15] E. Ideguchi, et al., *Phys. Rev. C* 94 (2016) 064322.
- [16] R. Yokoyama, et al., *Phys. Rev. C* 95 (2017) 034313.
- [17] Z. Patel, et al., *Phys. Rev. C* 96 (2017) 034305.
- [18] G.D. Dracoulis, P.M. Walker, F.G. Kondev, *Rep. Prog. Phys.* 79 (2016) 076301.
- [19] S. Nishimura, *Prog. Theor. Exp. Phys.* (2012) 03C006.
- [20] R.V.F. Janssens, F.S. Stephens, *Nucl. Phys. News* 6 (1996) 9.
- [21] N. Fukuda, et al., *Nucl. Instrum. Methods B* 317 (2013) 323.
- [22] H. Watanabe, et al., *Phys. Rev. Lett.* 113 (2014) 042502.
- [23] P.-A. Söderström, et al., *Nucl. Instrum. Methods B* 317 (2013) 649.
- [24] G.D. Dracoulis, et al., *Phys. Rev. C* 81 (2010) 054313.
- [25] J.J. Liu, submitted for publication.
- [26] G.X. Zhang, in preparation.
- [27] M. Asai, et al., *Phys. Rev. C* 59 (1999) 3060–3065.
- [28] P.-A. Söderström, et al., *Phys. Rev. C* 81 (2010) 034310.
- [29] <http://www.nndc.bnl.gov/ensdf/>.
- [30] T. Kibédi, et al., *Nucl. Instrum. Methods A* 589 (2008) 202.
- [31] L. Kostov, et al., *Nucl. Phys. A* 406 (1983) 541.
- [32] R. Nordhagen, R. Diamond, F. Stephens, *Nucl. Phys. A* 138 (1969) 231.
- [33] W. Andrejtscheff, et al., *Tech. Rep. ZfK-621,P40*, 1987.
- [34] F.G. Kondev, G.D. Dracoulis, T. Kibédi, *At. Data Nucl. Data Tables* 103–104 (2015) 50.
- [35] J. Bartel, et al., *Nucl. Phys. A* 386 (1) (1982) 79.
- [36] P. Walker, et al., *Nucl. Phys. A* 343 (1980) 45.
- [37] D.G. Burke, B. Elbek, *Kgl. Danske Vid. Selsk., Mat.-Fys. Medd.* 36 (6) (1967).
- [38] P.O. Tjøm, B. Elbek, *Nucl. Phys. A* 107 (1968) 385.
- [39] I.M. Govil, H.W. Fulbright, D. Cline, *Phys. Rev. C* 36 (1987) 1442.
- [40] K. Jain, et al., *Nucl. Phys. A* 591 (1995) 61.
- [41] W. Nazarewicz, et al., *Nucl. Phys. A* 435 (1985) 397.
- [42] C.J. Gallagher, S.A. Moszkowski, *Phys. Rev.* 111 (1958) 1282.
- [43] C.J. Orth, M.E. Bunker, J.W. Starner, *Phys. Rev.* 132 (1963) 355.
- [44] H. Morinaga, T. Yamazaki, *In-Beam Gamma-Ray Spectroscopy*, North-Holland Pub. Co., 1976.
- [45] M.E. Bunker, C.W. Reich, *Rev. Mod. Phys.* 43 (1971) 348.